Stability of Ships in Parametric Roll Resonance Under Time-Varying Heading and Speed

Dominik A. Breu, *Centre for Ships and Ocean Structures, Norwegian University of Science and Technology, Norway* breu@itk.ntnu.no

Christian Holden, *Department of Engineering Cybernetics, Norwegian University of Science and Technology, Norway* c.holden@ieee.org

Thor I. Fossen, *Department of Engineering Cybernetics, Norwegian University of Science and Technology, Norway* fossen@ieee.org

ABSTRACT

In this work, we derive an analytical 1-DOF roll model which is able to describe the dynamics of a ship in parametric resonance. We extend previous results to allow for slowly time-varying heading angle and speed. The hydrostatic and hydrodynamic model coefficients are identified based on simulations of an accurate 6-DOF ship model which accounts for first-order generalized pressure forces and moments by numerical integration of the instantaneous pressure field of the surrounding ocean over the instantaneous submerged hull. We determine functional expressions for the hydrodynamic coefficients which are dependent on the heading angle, resulting in an analytical 1-DOF roll model that is suitable for mathematical analysis and control purposes. We verify the model against the 6-DOF ship model in simulations.

Keywords: *Roll stability, Parametric roll, Nonlinear system, Time-varying system, Automatic control*

1. INTRODUCTION

Parametric roll resonance is a dangerous resonance phenomenon that has the ability to cause extreme roll angles for a wide range of ship types. Parametric roll resonance occurs in head or stern seas, with long-crested waves. The waves cause large changes in the ship's water plane area, resulting in a time-varying restoring term in roll. This effectively renders roll unstable as long as the encounter frequency is within a certain (ship-specific) range. Roll angles of over 40° have been observed on real ships. (Carmel, 2006; France et al., 2001; Galeazzi, 2009; Holden, 2011)

The effect of static encounter frequencies has been extensively investigated (ABS, 2004). Significantly less research has been done on the effects of time-varying encounter frequencies (Holden, 2011). The encounter frequency (the frequency of the waves as seen from the ship) can be changed via the Doppler effect. In practice, this can be done by changing the velocity of the ship relative to the waves. For most ships, this would be done by changing the surge speed and/or the course angle.

In Breu et al. (2012); Holden et al. (2012), a 6-degree-of-freedom (DOF) and a simplified 1-DOF model for ships in parametric roll with time-varying forward speed was presented and analyzed. The simplified model was also used to stabilize the roll angle by means of changing the forward speed, but not the course.

Changing the course can have adverse effects on the ship. When sailing in head seas, the ship

would not greatly suffer directly induced roll (but could be susceptible to parametric roll) (Holden, 2011). However, changing the course too much would potentially make the ship vulnerable to directly induced roll motion. If the course is changed too little, the ship will still be susceptible to parametric roll resonance. Great care must therefore be used when changing course during parametric roll resonance. These issues have not been extensively addressed by the research community (Holden, 2011).

In this work, we analyze the 6-DOF and 1-DOF models under both time-varying forward speed and yaw angle. The 1-DOF model is extended to incorporate non-constant yaw angles and the model parameters are identified by curve fitting. Stability regions are investigated in simulations.

The remainder of this paper is organized as follows: Section 2 summarizes the 6-DOF ship model as used in Breu et al. (2012). Section 3 presents the extended 1-DOF roll model which is able to handle both time-varying speed and time-varying heading angles. In Section 4, the hydrostatic and the hydrodynamic coefficients of the 1-DOF roll model are identified and the model is verified in Section 5. Section 6 contains the conclusion.

2. 6-DOF SHIP MODEL

In Breu et al. (2012), we derived a highly accurate 6-DOF ship model of a container ship which accounts for the first-order external forces and moments on the ship due to the hydrostatic and hydrodynamic pressure field of the ocean. The ship model is numerical, and the instantaneous ocean pressure is integrated over the instantaneous submerged hull at each time step. This gives the generalized external forces and generalized restoring forces (except gravity) on the ship.

The 6-DOF ship model is given by (Breu et al., 2012; Fossen, 2011)

$$\dot{\boldsymbol{\eta}} = \mathbf{J}(\boldsymbol{\Theta})\,\mathbf{v} \tag{1}$$

$$\mathbf{M}\dot{\mathbf{v}} + \mathbf{D}(\mathbf{v})\mathbf{v} + \mathbf{C}(\mathbf{v})\mathbf{v} + \mathbf{k}(\boldsymbol{\eta},t) = \boldsymbol{\tau}_c + \boldsymbol{\tau}_e \tag{2}$$

where the ship's generalized position vector $\boldsymbol{\eta} = \left[\mathbf{p}^{n\top}, \boldsymbol{\Theta}^{\top}\right]^{\top} \in \mathbb{R}^6$ consists of its position in the inertial frame $\mathbf{p}^n = \left[x^n, y^n, z^n\right]^{\top} \in \mathbb{R}^3$ and the vector of Euler angles $\boldsymbol{\Theta} = \left[\phi, \theta, \psi\right]^{\top} \in \mathbb{R}^3$ which represents its rotation relative to the inertial reference frame. The ship's generalized velocity vector is denoted by $\mathbf{v} = \left[\mathbf{v}^{b\top}, \boldsymbol{\omega}^{b\top}\right]^{\top} \in \mathbb{R}^6$ where $\mathbf{v}^b = \left[u, v, w\right]^{\top} \in \mathbb{R}^3$ is the ship's linear and $\boldsymbol{\omega}^b = \left[p, q, r\right]^{\top} \in \mathbb{R}^3$ the angular velocity vector, both expressed in a body-fixed reference frame. The transformation matrix $\mathbf{J} \in \mathbb{R}^{6\times 6}$ transforms the body-fixed velocities into inertial reference frame velocities and is as defined in Fossen (2011).

The sum of the rigid-body inertia and added mass is denoted by $\mathbf{M} \in \mathbb{R}^{6\times 6}$ in (2), whereas $\mathbf{D} \in \mathbb{R}^{6\times 6}$ and $\mathbf{C} \in \mathbb{R}^{6\times 6}$ are the damping and the Coriolis/centripetal matrices, respectively. The generalized control forces are $\boldsymbol{\tau}_c \in \mathbb{R}^6$ and the generalized forces due to environmental disturbances other than waves are $\boldsymbol{\tau}_e \in \mathbb{R}^6$ (wave effects are included in $\mathbf{k}$). The model is equipped with a simple PID controller to maintain course and surge speed.

$\mathbf{k} = \mathbf{k}_p + \mathbf{k}_g \in \mathbb{R}^6$ is the sum of the generalized pressure and the gravity forces where the latter are given by Fossen (2011)

$$\mathbf{k}_g(\boldsymbol{\eta}) = -mg \begin{bmatrix} \mathbf{R}^{\top}(\boldsymbol{\Theta})\,\mathbf{e}_z \\ \left(\mathbf{R}^{\top}(\boldsymbol{\Theta})\,\mathbf{e}_z\right) \times \mathbf{r}_g^b \end{bmatrix}. \tag{3}$$

Here, $\mathbf{r}_g^b \in \mathbb{R}^3$ is the ship's center of gravity in the body-fixed reference frame, $\mathbf{e}_z = \left[0,0,1\right]^{\top}$, m the ship's mass, and g the acceleration of

gravity. The rotation matrix $\mathbf{R} \in \mathbb{R}^{3\times3}$ is as defined in Fossen (2011).

$\mathbf{k}_p$ is computed by integrating the instantaneous pressure over the instantaneous submerged hull, under the assumption that the ocean pressure field is unchanged by the passage of the ship (the waves are effectively traveling "through" the vessel). We assume that the ship's hull consists of sections, and that each section can be parameterized with parameters a and b. We let the position of a point on the surface of the panel i in the body-fixed reference frame be $\mathbf{r}_i^b(a,b) \in \mathbb{R}^3$. The local pressure field at any given point $\mathbf{r}^n \in \mathbb{R}^3$ in the ocean is, under the same assumptions as in Breu et al. (2012), $\Psi \approx \Psi(\mathbf{r}^n, t) \in \mathbb{R}$ (Faltinsen, 1998; Perez, 2005). By defining

$$\Psi_i(a,b) \triangleq \Psi\left(\mathbf{R}\mathbf{r}_i^b(a,b) + \mathbf{x}^n, t\right), \qquad (4)$$

the generalized pressure forces of the surrounding ocean on the ship are (Perez, 2005; White, 2002)

$$\mathbf{k}_p(\boldsymbol{\eta}, t) = \sum_i \begin{bmatrix} f_i \\ g_i \end{bmatrix} \qquad (5)$$

where

$$f_i = \int_{S_{w,i}} \Psi_i(a,b) \frac{\partial \mathbf{r}_i^b}{\partial a}(a,b) \times \frac{\partial \mathbf{r}_i^b}{\partial b}(a,b)\, \mathrm{d}a\, \mathrm{d}b$$

$$g_i = \int_{S_{w,i}} \Psi_i(a,b) \mathbf{r}_i^b(a,b) \times \left(\frac{\partial \mathbf{r}_i^b}{\partial a}(a,b) \times \frac{\partial \mathbf{r}_i^b}{\partial b}(a,b) \right) \mathrm{d}a\, \mathrm{d}b$$

are the forces and moments on panel i due to the pressure of the surrounding ocean. The wetted part of panel i is $S_{w,i}$ and the ship is parameterized so that the normal vector $(\partial \mathbf{r}_i^b / \partial a) \times (\partial \mathbf{r}_i^b / \partial b)$ points out of the hull. The generalized force $\mathbf{k}_p$ accounts for all the effects of current and waves (Faltinsen, 1998; Perez, 2005).

Note that the pressure forces are not the same as the Froude-Krylov force, although made under somewhat similar assumptions, as the force used in the 6-DOF model – unlike the Froude-Krylov force – is computed based on numerical integration of the instantaneous submerged hull.

Refer to Breu et al. (2012) for further details of the calculation of the generalized pressure forces.

3. 1-DOF ROLL MODEL

The complex 6-DOF ship model (1) and (2) of Section 2 is a numerical model which relies on the integration of the hydrodynamic and hydrostatic pressure field over the instantaneous submerged part of the hull. Though the 6-DOF model is highly suitable for simulation studies, its usability for control purposes and mathematical analysis is limited.

In Breu et al. (2012), we considered the three most important degrees of freedom for a ship in parametric roll resonance, that is, the heave, roll and pitch motions. By using a quasi-steady approach we derived an analytical 1-DOF roll model – a model with an explicit functional (rather than a numerical) relationship between time and wave force – which accurately captured the parametric roll motion of a ship. However, the 1-DOF model in Breu et al. (2012) assumed that only the ship's surge speed could change, while the heading angle was assumed constant.

In this section, we will derive an analytical 1-DOF roll model where the ship's speed and heading angle are allowed to be time-varying, if only slowly. For a large ship, like many ships susceptible to parametric roll (Holden, 2011), this is a reasonable assumption.

Motivated by the model introduced in Breu et al. (2012) and following the same derivation, we tentatively choose the 1-DOF roll model as

$$\begin{aligned} &m_{44}\ddot{\phi}+d_{44}\dot{\phi}+\kappa_2\cos\left(\int_{t_0}^{t}\omega_e(\tau)\,\mathrm{d}\tau+\kappa_3\right)\phi \\ &+\kappa_1\phi+\kappa_4\phi^3=\kappa_5\sin\left(\int_{t_0}^{t}\omega_e(\tau)\,\mathrm{d}\tau+\kappa_6\right) \end{aligned} \tag{6}$$

where m_{44} is the sum of the rigid-body moment of inertia and the added moment of inertia in roll and d_{44} is the linear damping coefficient in roll. The linear and the cubic restoring coefficients in roll are κ_1 and κ_4, respectively. Those are hydrostatic coefficients and thus assumed constant. The coefficients $\kappa_i=\kappa_i(u,\psi)$, $i\in\{2,3,5,6\}$, may be dependent on the ship's surge speed and heading angle or both (e.g., $\kappa_5\approx 0$ for head seas).

For simplicity, we assume that the waves are traveling along the inertial x-axis, and are sinusoidal.

The encounter frequency ω_e is the frequency of the waves perceived by an observer moving with the ship. Essentially, the encounter frequency is the Doppler-shifted wave frequency due to the non-zero speed of the ship, and it can be expressed as (Breu et al., 2012)

$$\begin{aligned} \omega_e &= \frac{\mathrm{d}}{\mathrm{d}t}\left(\omega_0 t-k_w\int_{t_0}^{t}u^n(\tau)\,\mathrm{d}\tau\right) \\ &\approx \omega_0-k_w\cos(\psi)u \end{aligned} \tag{7}$$

where ω_0 is the modal wave frequency, k_w the wave number as seen in the inertial frame and u^n is the ship's speed along the inertial x-axis. It is evident from (7) that the encounter frequency is dependent on both the ship's surge speed and the heading angle.

The model introduced in Breu et al. (2012) and the 1-DOF roll model (6) differ in three major aspects. Whereas the model in Breu et al. (2012) assumes constant coefficients, most of the model coefficients in (6) are explicitly allowed to be dependent on the ship's surge speed and heading angle. Furthermore, the model (6) incorporates directly excited roll motion by considering the external forcing term on the right hand side of (6) (the Froude-Krylov force (Perez, 2005)) which was neglected in Breu et al. (2012) due to the ship sailing in head sea conditions. Finally, in Breu et al. (2012), $\dot{\psi}\equiv 0$ and $\dot{u}\not\equiv 0$. Here, $\dot{\psi}\not\equiv 0$ and $\dot{u}\not\equiv 0$.

4. MODEL COEFFICIENT IDENTIFICATION

In this section, the coefficients κ_i, $i\in\{1,\ldots,6\}$ of the 1-DOF roll model (6) will be identified from simulations of the 6-DOF model (1) and (2).

The hydrostatic coefficients κ_1 and κ_4 are constants, and they can be determined from simulations without waves. κ_2 and κ_3 are the coefficients of the change in the amplitude of the linear restoring moment in roll and its phase due to the passage of the waves, and account for the coupling of roll to the heave and pitch motions. The external wave forcing is considered by the right hand side of (6) with its hydrodynamic coefficients κ_5 and κ_6.

4.1 Hydrostatic Coefficients

The constant coefficients κ_1 and κ_4 are found by a free decay test. Define the spring torque for the 1-DOF roll model (6) without wave influence as

$$k_{\bar{\phi}}(t;\bar{\kappa})=\kappa_1\phi(t)+\kappa_4\phi^3(t). \tag{8}$$

The hydrostatic coefficient vector $\bar{\kappa}=[\kappa_1,\kappa_4]$ is identified by a nonlinear least-square curve fitting of (8) to the pressure-induced

generalized forces in roll of the 6-DOF model (1) and (2) simulated in a calm water scenario. Thus, by denoting the fourth element of $\mathbf{k}$ in (2) as $k^{\{4\}}$, $\bar{\kappa}$ is given by

$$\bar{\kappa} = \arg\min_{\bar{\kappa}} \sum_t \left| k^{\{4\}}\left(\boldsymbol{\eta}(t), t\right) - k_{\bar{\phi}}\left(t; \bar{\kappa}\right) \right|^2 \qquad (9)$$

4.2 Hydrodynamic Coefficients

The identification of the hydrodynamic coefficients $\tilde{\kappa} = [\kappa_2, \kappa_3, \kappa_5, \kappa_6]$ is done in the following way:

The complex 6-DOF model is simulated for a wide range of constant u, ψ doubles, and the pressure-induced moment in roll (the fourth element of $\mathbf{k}$, that is $k^{\{4\}}$) is saved. We define the sum of the restoring and external moments in roll as

$$k_\phi(t;\kappa) = \left[\kappa_1 + \kappa_2 \cos\left(\int_{t_0}^{t} \omega_e(\tau)\,\mathrm{d}\tau + \kappa_3 \right) \right] \phi(t) + \kappa_4 \phi^3(t) - \kappa_5 \sin\left(\int_{t_0}^{t} \omega_e(\tau)\,\mathrm{d}\tau + \kappa_6 \right). \qquad (10)$$

The coefficients $\tilde{\kappa}$ for these conditions are then found as

$$\tilde{\kappa} = \arg\min_{\tilde{\kappa}} \sum_t \left| k^{\{4\}}\left(\boldsymbol{\eta}(t), t\right) - k_\phi\left(t; \kappa\right) \right|^2 \qquad (11)$$

where we use the values of the hydrostatic coefficients κ_1 and κ_4 found from the free decay tests in Section 4.1. This procedure results in one set of $\tilde{\kappa}$s per u, ψ double. The parameters for the simulations of the 6-DOF ship model are equivalent to the ones presented in Breu et al. (2012).

Figures 1–4 show the results of this procedure for surge speeds u ranging from $0\,\mathrm{m/s}$ to $10\,\mathrm{m/s}$ and for heading angles ψ from 0° to 90°. Note that heading angles of 0° and 90° correspond to the ship sailing in head sea and beam sea conditions.

The hydrodynamic coefficient κ_6 represents the phase angle of the external sinusoidal wave force. Note that, in head sea conditions ($\psi = 0°$) the amplitude of the external forcing term is zero which can be observed in Figure 3. As a consequence κ_6 cannot be estimated in those conditions.

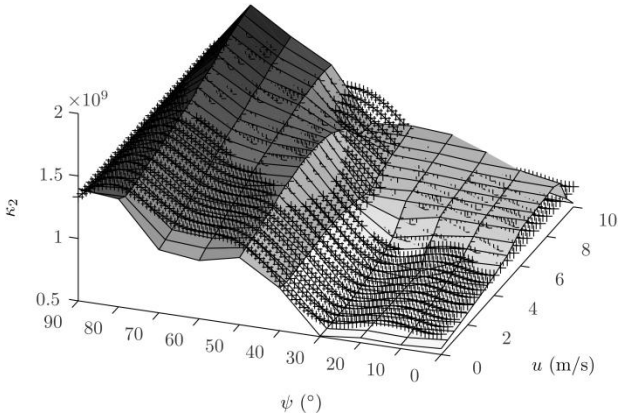

Figure 1: Hydrodynamic coefficient κ_2 and its functional approximation (denoted by +)

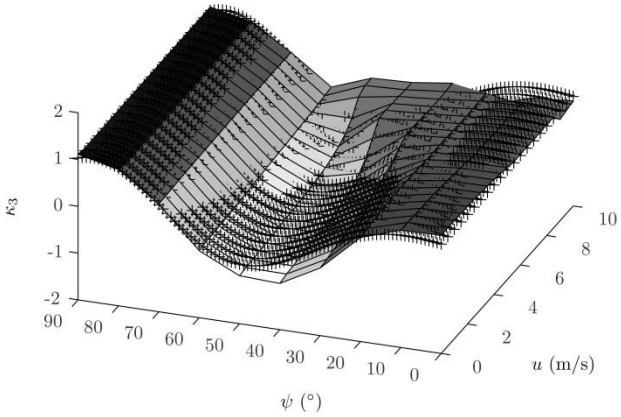

Figure 2: Hydrodynamic coefficient κ_3 and its functional approximation (denoted by +)

4.3 Identification of $\tilde{\kappa}$

We desire a functional expression for the coefficients $\tilde{\kappa}$ for a wide range of surge speeds and heading angles. This allows the analytical analysis of the roll, giving both easier analysis and better simulation than a numerical model.

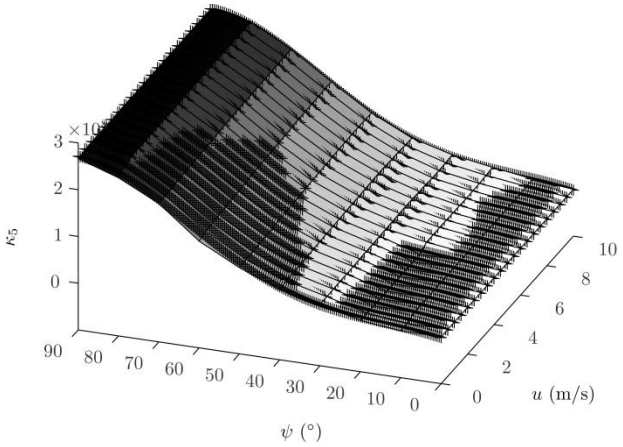

Figure 3: Hydrodynamic coefficient κ_5 and its functional approximation (denoted by +)

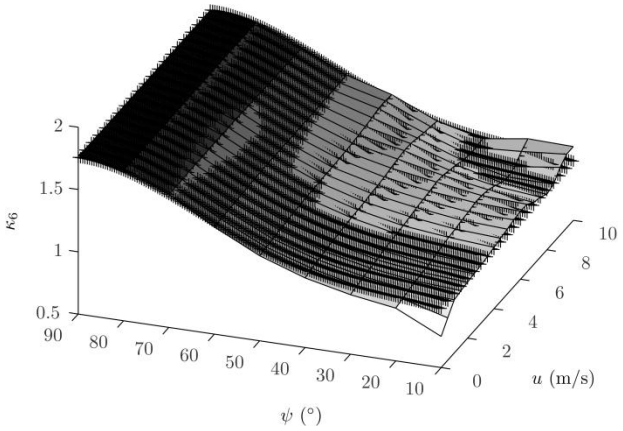

Figure 4: Hydrodynamic coefficient κ_6 and its functional approximation (denoted by +)

We use the values of $\tilde{\kappa}$ obtained in Section 4.2 to derive a functional relationship between ψ and u and $\tilde{\kappa}$. From Figures 1–4, it appears that $\tilde{\kappa}$ predominantly varies with the heading angle ψ, not the surge speed u. Furthermore, the relationship appears to be sinusoidal in nature. We therefore use the following functions for $\tilde{\kappa}$:

$$\begin{aligned}\kappa_2 = \kappa_2(\psi) &= \varkappa_{2,1}\sin\left(\varkappa_{2,2}\psi + \varkappa_{2,3}\right) \\ &+\varkappa_{2,4}\sin\left(\varkappa_{2,5}\psi + \varkappa_{2,6}\right) \\ &+\varkappa_{2,7}\sin\left(\varkappa_{2,8}\psi + \varkappa_{2,9}\right)\end{aligned} \tag{12}$$

$$\begin{aligned}\kappa_3 = \kappa_3(\psi) &= \varkappa_{3,1}\sin\left(\varkappa_{3,2}\psi + \varkappa_{3,3}\right) \\ &+\varkappa_{3,4}\sin\left(\varkappa_{3,5}\psi + \varkappa_{3,6}\right)\end{aligned} \tag{13}$$

$$\begin{aligned}\kappa_5 = \kappa_5(\psi) &= \varkappa_{5,1}\sin\left(\varkappa_{5,2}\psi + \varkappa_{5,3}\right) \\ &+\varkappa_{5,4}\sin\left(\varkappa_{5,5}\psi + \varkappa_{5,6}\right)\end{aligned} \tag{14}$$

$$\begin{aligned}\kappa_6 = \kappa_6(\psi) &= \varkappa_{6,1}\sin\left(\varkappa_{6,2}\psi + \varkappa_{6,3}\right) \\ &+\varkappa_{6,4}\sin\left(\varkappa_{6,5}\psi + \varkappa_{6,6}\right).\end{aligned} \tag{15}$$

To determine the parameter values for $\tilde{\kappa}$, we curve fit the above functions to the data gathered for $\tilde{\kappa}$ in the first step in Section 4.2. The results of the curve fitting of the functions (12)–(15) are shown in Figures 1–4 (denoted by + in the plots).

The coefficients κ_5 and κ_6, corresponding to the external wave forcing, are very well approximated by the functional expressions (14) and (15). On the other hand, the approximations of κ_2 and κ_3 which account for the coupling of roll to the heave and pitch motion, are less accurately described by (12) and (13). Mainly for large surge speeds and small heading angles, there is a discrepancy between the hydrodynamic coefficients and its functional approximations. In Section 5 it will become evident that this corresponds to when the ship is experiencing parametric roll resonance. However, we will show that the functional expressions for κ_2 and κ_3 are appropriate to describe the roll dynamics to a satisfactory extent.

5. MODEL VERIFICATION

In this section, we verify the 1-DOF roll model of Section 3 with the hydrodynamic coefficients given by the functional expressions presented in Section 4.3. To that matter, we simulate the 1-DOF roll model and compare it to simulations of the complex 6-DOF model of Section 2. The simulations are performed using the same model parameters as in Breu et al. (2012).

5.1 Maximum Roll Angle

We simulate the 6-DOF ship model (1) and (2) for a wide range of surge speeds and heading angles. For each simulation, the surge speed and the heading angle are kept constant (except for small variations due to the limited bandwidth of the speed and heading controllers). Then, we simulate the 1-DOF roll model (6) where the surge speed and heading angle of the previous simulations of the 6-DOF model enter via the encounter frequency (7). The maximum steady-state roll angles of the various simulation scenarios for the different models are depicted in Figures 5–7.

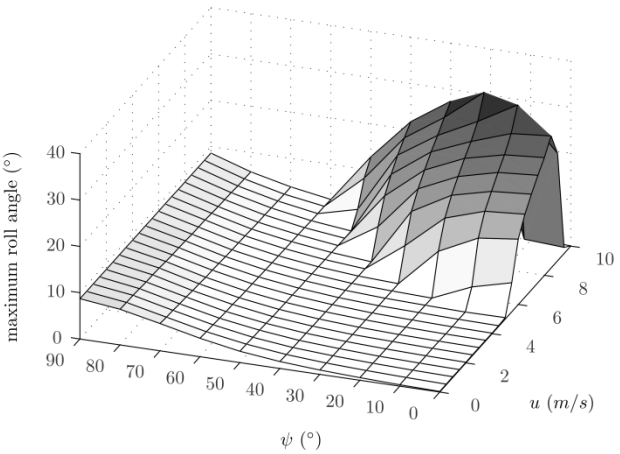

Figure 5: Maximum roll angle, 6-DOF model

From the simulations of the 6-DOF ship model depicted in Figure 5, it is evident that the ship is experiencing parametric roll resonance of up to 30° for large surge speeds and small heading angles. This corresponds to an encounter frequency which is close to twice the natural roll frequency, a well-known criteria for parametric resonance (Nayfeh and Mook, 1995).[1]

Furthermore, it is noticeable from Figure 5 that the ship is suffering directly excited roll motions at high heading angles, independent of the surge speed. Those maximum roll angles are considerably lower than the maximum roll angles caused by parametric resonance and peak in beam sea condition.

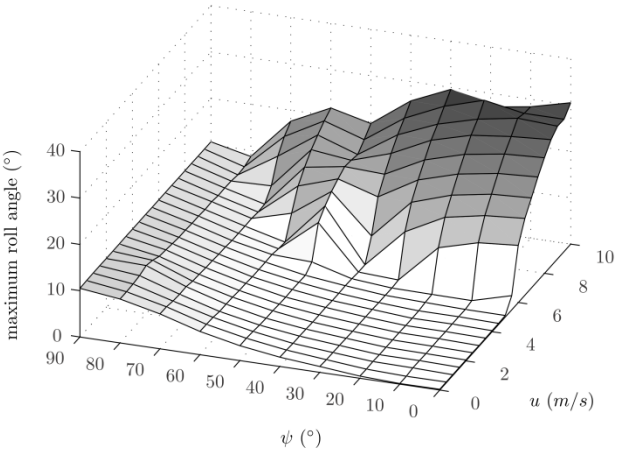

Figure 6: Maximum roll angle, 1-DOF model

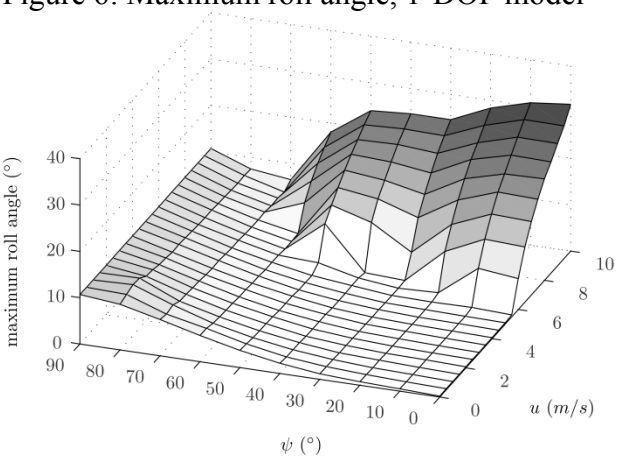

Figure 7: Maximum roll angle, 1-DOF model, functional expressions

Figure 6 depicts the simulation results from the 1-DOF roll model where the hydrodynamic coefficients are determined numerically from the simulations of the 6-DOF model for each simulation scenario. In Figure 7 the maximum roll angles are shown for the 1-DOF model with the hydrodynamic coefficients approximated by the functional expressions of Section 4.3.

The plots of the maximum roll angles in Figures 6 and 7 are very similar. That indicates that the functional approximation of the hydrodynamic model coefficients of Section 4.3 is appropriate.

Comparing the simulations of the 1-DOF roll models in Figures 6 and 7 to the simulations of the 6-DOF model depicted in Figure 5, the 1-

[1] The apparent higher roll angle for low, non-zero heading angles might be due to low speed resolution in the border between parametric roll and not parametric roll.

DOF roll models are qualitatively quite close to the 6-DOF model for most of the simulation scenarios. The maximum roll angle is slightly overestimated by the 1-DOF models; however that may be explained by the simplifications in the derivation of the 1-DOF models and lack of higher-order restoring coefficients.

However, for the 1-DOF roll models, the region of parametric roll resonance at large surge speeds extends to higher heading angles than for the 6-DOF model. This is slightly less pronounced for the 1-DOF model with the functional expressions for the coefficients.

This effect is probably caused by two effects: The assumption of speed independence of κ_2 and κ_3 breaks down when the speed range is very large (see Figs 1 and 2); and the behavior at the borders of the area of parametric resonance – especially the non-smooth borders – is difficult to model accurately.

5.2 Time-Varying Heading and Speed

Since the 1-DOF roll model (6) with functional expressions for the hydrodynamic coefficients was derived to allow time-varying heading angle and surge speed, we simulate it for non-constant heading and speed. The results are compared to simulations of the full 6-DOF ship model (1) and (2).

The initial conditions of the simulation scenario are chosen such that the ship is in parametric roll resonance condition, specifically $\psi(0) = 0$, $u(0) = 7\mathrm{m/s}$. At 200s the surge speed is increased gradually to about $8\mathrm{m/s}$ with a constant acceleration of $0.005\mathrm{m/s^2}$ while the heading angle is increased by $0.1°/\mathrm{s}$ to approximately 20°. The surge speed and the heading angle are depicted in Figures 9 and 10, respectively. The oscillations in surge and yaw are due to the limited bandwidth of the PID controllers.

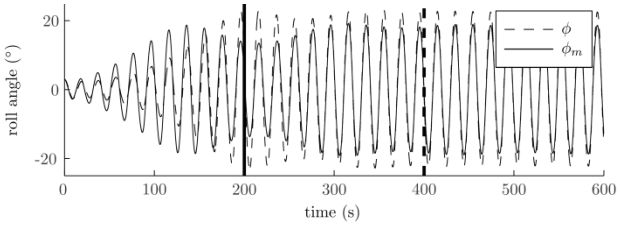

Figure 8: Roll angle

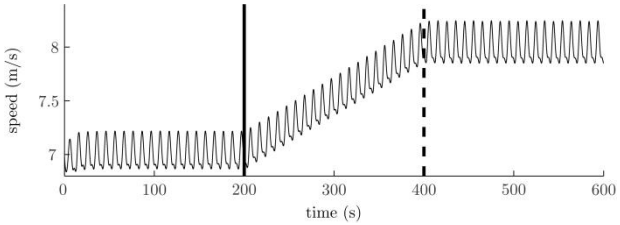

Figure 9: Speed

Figure 8 shows the roll angle of the 6-DOF model ϕ and of the 1-DOF model ϕ_m. The ship is experiencing large roll amplitudes up to about 20° due to parametric roll resonance. The roll angle of the 1-DOF model is qualitatively very close to that of the 6-DOF model, being only slightly underestimated. The sum of the restoring and external moments in roll are depicted in Figure 11, and they show a good match between the 6-DOF model and the 1-DOF model.

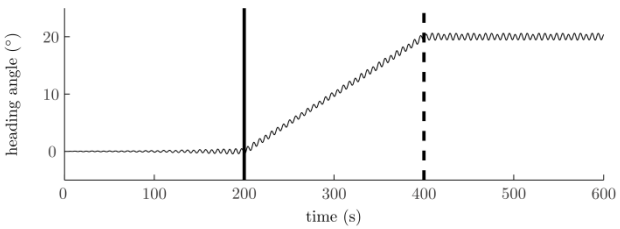

Figure 10: Heading angle

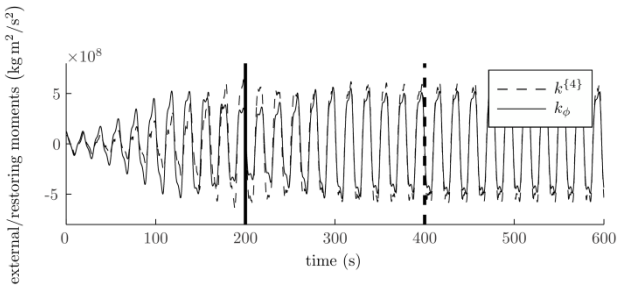

Figure 11: Restoring/ external moments in roll

The simulation scenario with time-varying speed and heading angle indicates that the 1-

DOF model with the hydrodynamic coefficients given by heading dependent functions is appropriate to describe the ship's dynamics during parametric roll resonance.

6. CONCLUSIONS

In this work, we have derived a 1-DOF roll model for ships in parametric roll resonance. We have extended the model of previous works to incorporate both slowly time-varying heading angle and surge speed. The proposed 1-DOF roll model is based on the explicit time-solutions of the heave and pitch motions by a quasi-steady approach.

The hydrodynamic coefficients of the 1-DOF roll model are identified from a complex and accurate 6-DOF model of a container ship for certain fixed surge speeds and heading angles. The 6-DOF model, which accounts for first-order generalized pressure forces by integrating the instantaneous pressure field of the ocean numerically over the instantaneous submerged part of the ship hull.

Based on these parameters, we have found functional expressions for the hydrodynamic model coefficients dependent only on the heading angle. The parameters of those functions were found by curve fitting the hydrodynamic coefficients to the coefficients obtained by the 6-DOF ship model for a wide range of ship speeds and heading angles.

We have shown in simulations that the proposed 1-DOF roll model qualitatively describes the results of the 6-DOF model well for various speeds and heading angles and also captures the roll dynamics closely when the speed and the heading angle are time-varying.

ACKNOWLEDMENTS

This work was funded by the Centre for Ships and Ocean Structures and the Norwegian Research Council.

BIBLIOGRAPHY

ABS, 2004. “Assessment of Parametric Roll Resonance in the Design of Container Carriers.” Tech. rep., American Bureau of Shipping.

Breu, D. A., Holden, C., and Fossen, T. I., 2012. “Ship Model for Parametric Roll Incorporating the Effects of Time-Varying Speed.” Fossen, T. I. and Nijmeijer, H. (eds.), Parametric Resonance in Dynamical Systems, Springer, chap. 9. pp. 167–189.

Carmel, S. M., 2006. “Study of Parametric Rolling Event on a Panamax Container Vessel.” Journal of the Transportation Research Board, vol. 1963, pp. 56–63.

Faltinsen, O. M., 1998. Sea Loads on Ships and Offshore Structures. Cambridge University Press.

Fossen, T. I., 2011. Handbook of Marine Craft Hydrodynamics and Motion Control. Wiley.

France, W. N., Levadou, M., Treakle, T. W., Paulling, J. R., Michel, R. K., and Moore, C., 2001. “An investigation of head-sea parametric rolling and its influence on container lashing systems.” SNAME Annual Meeting.

Galeazzi, R., 2009. Autonomous Supervision and Control of Parametric Roll Resonance. Ph.D. thesis, Technical University of Denmark.

Holden, C., 2011. Modeling and Control of Parametric Roll Resonance. Ph.D. thesis, Norwegian University of Science and Technology.

Holden, C., Breu, D. A., and Fossen, T. I., 2012. “Frequency Detuning Control by Doppler Shift.” Fossen, T. I. and Nijmeijer, H. (eds.), Parametric Resonance in Dynamical Systems, Springer, chap. 10. pp. 193–212.

Nayfeh, A. H. and Mook, D. T., 1995. Nonlinear Oscillations. Wiley.

Perez, T., 2005. Ship Motion Control. Advances in Industrial Control. Springer-Verlag, London.

White, F. M., 2002. Fluid Mechanics. McGraw Hill Text.